

Supporting Information

Effect of alkyl spacer length of thienyl-substituted carbazole-type self-assembled monolayers on the performance of inverted perovskite solar cells

Nobuko Onozawa-Komatsuzaki,^{a*} Atsushi Kogo,^a Takuma Chigira,^{a,b} Hiroyuki Yaguchi,^b Masayuki Chikamatsu,^a Takashi Funaki^{a*} and Takuro N. Murakami^{a*}

^a*National Institute of Advanced Industrial Science and Technology (AIST),*

Central 5, 1-1-1 Higashi Tsukuba, Ibaraki 305-8565, Japan

^b*Graduate School of Science and Engineering, Saitama University, 255 Shimo-Okubo, Sakura-ku, Saitama 338-8570, Japan*

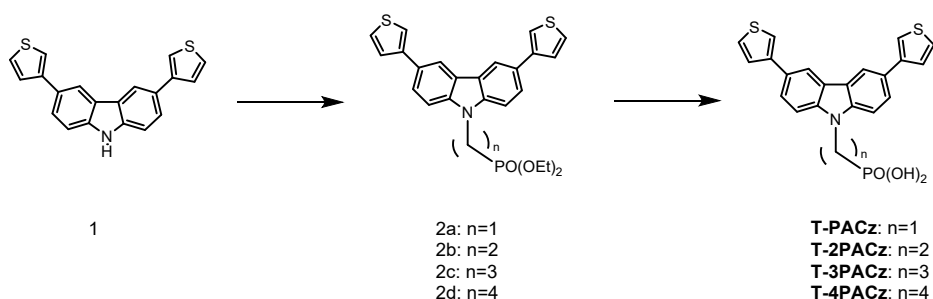
E-mail: n-onozawa@aist.go.jp

1. General information

All commercially available chemicals and solvents were used without further purification. ¹H NMR spectra were recorded on a Bruker Avance400 (400 MHz). Chemical shifts are given in ppm relative to standard (tetramethylsilane). The splitting patterns are designated as follows: s (singlet); d (doublet); t (triplet); q (quartet) and m

(multiplet). Column chromatography was performed on silica gel (Wako, wakosil-C200, spherica, 1, 64-210 μm).

2. Synthesis of thienyl substituted carbazole typed SAMs



Scheme S1. Synthesis of thiophen functionalized carbazole-type SAMs.

Synthesis of **1**

A mixture of 3,6-dibromocarbazole (3.00 g, 9.23 mmol), 3-thiopheneboronic acid (2.60 g, 20.3 mmol), tetrakis(triphenylphosphine)palladium(0) (1.07 g, 0.923 mmol) in 1,2-dimethoxyethane (75 mL) and 2 M Na_2CO_3 aqueous solution (75 mL) was refluxed for 4 h. After cooling to room temperature, the reaction mixture was extracted with CH_2Cl_2 (100 mL x 3) and dried over MgSO_4 . After the filtration of the organic layer, the filtration was concentrated *in vacuo*. The residue was purified by column chromatography (SiO_2 , CH_2Cl_2 and hexane) to give the desired compounds in 98.4 % yield (3.01 g). ^1H NMR

(400 MHz, CDCl₃, Me₄Si) δ 8.32 (2H, d, 1.8), 8.08 (1H, br), 7.69 (2H, dd, 8.4, 1.8), 7.52 (2H, dd, 4.9, 1.4), 7.49 (2H, dd, 3.0, 1.4), 7.46-7.42 (4H, m).

Synthesis of 2a

To a suspension of NaH (0.0543 g, 1.36 mmol) in THF (10 mL), **1** (0.300 g, 9.05 mmol) in DMF (7 mL) was added dropwise and the mixture was stirred at room temperature for 30 min. Afterwards diethyl(chloromethyl)phosphonate (0.253 g, 1.36 mmol) in dimethylformamide (DMF) (3 mL) was added dropwise to the mixture. The resulting solution was stirred at 80 °C for 29 h. After cooling to room temperature, the reaction mixture was extracted with CH₂Cl₂ (50 mL x 3) and dried over MgSO₄. After the filtration of the organic layer, the filtration was concentrated *in vacuo*. The residue was purified by column chromatography (SiO₂, CH₂Cl₂ and MeOH) to give the desired compounds in 17.2% yield (0.075 g). ¹H NMR (400 MHz, CDCl₃, Me₄Si) δ 8.32 (2H, dd, 1.8, 0.6), 7.76 (2H, dd, 6.2, 1.8), 7.54–7.50 (6H, m), 7.44 (2H, dd, 5.0, 3.0), 4.69 (1H, s), 4.67 (1H, s), 4.02-3.96 (4H, m), 1.16 (6H, t, 7.1).

Synthesis of 2b

2b was prepared following the method of **2a**, from **1** (8.00 g, 24.1 mmol), NaH (1.45 g, 36.2 mmol), diethyl 2-bromoethylphosphonate (8.87 g, 36.2 mmol), in tetrahydrofuran (THF) (200 mL) and DMF (200 mL) to give the desired compounds in 97.7% yield (11.7 g). ¹H NMR (400 MHz, CDCl₃, Me₄Si) δ 8.33 (2H, d, 1.7), 7.75 (2H, dd, 8.4, 1.7), 7.52

(2H, dd, 5.0, 1.4), 7.49 (2H, dd, 2.9, 1.4), 7.47–7.43 (4H, m), 4.67-4.61 (2H, m), 4.12–4.05 (4H, m), 2.35–2.27 (2H, m), 1.29 (6H, t, 7.1).

Synthesis of **2c**

2c was prepared following the method of **2a**, from **1** (1.00 g, 3.02 mmol), NaH (0.181 g, 4.53 mmol), diethyl 3-bromopropylphosphonate (1.17 g, 4.53 mmol), in THF (20 mL) and DMF (20 mL) to give the desired compounds in 100% yield (1.54 g). ¹H NMR (400 MHz, CDCl₃, Me₄Si) δ 8.34 (2H, d, 1.7), 7.74 (2H, dd, 8.4, 1.7), 7.53 (2H, dd, 4.9, 1.4), 7.50-7.43 (6H, m), 4.45 (2H, t, 7.1), 4.14–4.02 (4H, m), 2.29-2.18 (2H, m), 1.82–1.74 (2H, m), 1.29 (6H, t, 7.1).

Synthesis of **2d**

2d was prepared following the method of **2a**, from **1** (1.00 g, 3.02 mmol), NaH (0.181 g, 4.53 mmol), diethyl 4-bromobutylphosphonate (1.24 g, 4.53 mmol), in THF (20 mL) and DMF (20 mL) to give the desired compounds in 96.2% yield (1.52 g). ¹H NMR (400 MHz, CDCl₃, Me₄Si) δ 8.34 (2H, dd, 1.8, 0.7), 7.73 (2H, dd, 8.4, 1.8), 7.52 (2H, dd, 4.9, 1.4), 7.49 (2H, dd, 3.0, 1.4), 7.45-7.41 (4H, m), 4.35 (2H, t, 7.1), 4.07–3.99 (4H, m), 2.06-1.99 (2H, m), 1.77–1.69 (4H, m), 1.25 (6H, t, 7.1).

Synthesis of T-PACz

A mixture of **2a** (0.300 g, 0.623 mmol) and bromotrimethylsilane (0.477 g, 3.11 mmol) in CH₂Cl₂ (60 mL) stirred at room temperature for 4 days. MeOH (30 mL) was added to the reaction mixture and stirred further 3 h at room temperature. After the solvent was evaporated *in vacuo*, solid residue was suspended to water. The mixture was filtrated and washed with water. The crude product was purified by recrystallization (EtOH) to give the desired compounds in 70.2 % yield (0.186 g). ¹H NMR (400 MHz, dimethyl sulfoxide (DMSO)-*d*₆, Me₄Si) δ 8.59 (2H, d, 1.7), 7.84–7.82 (4H, m), 7.70–7.66 (4H, m), 7.61 (2H, d, 8.6), 4.65 (1H, s), 4.62 (1H, s).

Synthesis of T-2PACz

T-2PACz was prepared following the method of **T-PACz**, from **2b** (1.00 g, 2.02 mmol), bromotrimethylsilane (0.680 g, 4.44 mmol), CH₂Cl₂ (10 mL), and MeOH (5 mL) to give the desired compounds in 91.5 % yield (0.812 g). ¹H NMR (400 MHz, DMSO-*d*₆, Me₄Si) δ 8.62 (2H, d, 1.8), 7.88–7.85 (4H, m), 7.70–7.67 (4H, m), 7.57 (2H, d, 8.6), 4.60–4.54 (2H, m), 2.11–2.02 (2H, m).

Synthesis of T-3PACz

T-3PACz was prepared following the method of **T-PACz**, from **2c** (1.50 g, 2.94 mmol), bromotrimethylsilane (0.991 g, 6.48 mmol), CH₂Cl₂ (15 mL), and MeOH (30 mL) to give the desired compounds in 59.3 % yield (0.789 g). ¹H NMR (400 MHz, DMSO-*d*₆, Me₄Si) δ 8.62 (2H, d, 1.8), 7.86–7.83 (4H, m), 7.71–7.67 (6H, m), 4.52 (2H, t, 8.9), 2.04–1.97 (2H, m), 1.59–1.51 (2H, m).

Synthesis of T-4PACz

T-4PACz was prepared following the method of T-PACz, from **2d** (1.45 g, 2.77 mmol), bromotrimethylsilane (2.12 g, 13.8 mmol), CH₂Cl₂ (140 mL), and MeOH (90 mL) to give the desired compounds in 24.0 % yield (0.309 g). ¹H NMR (400 MHz, DMSO-*d*₆, Me₄Si) δ 8.61 (2H, d, 1.8), 7.85–7.82 (4H, m), 7.70–7.64 (6H, m), 4.43 (2H, t, 7.0), 1.92–1.85 (2H, m), 1.56–1.53 (4H, m)

3. Cyclic voltammetry (CV) of thin films

CV of thin film was performed on an ALS/610B electrochemical analyzer with the CV cell consisting of a bare or hole collecting monolayer adsorbed ITO working electrode, a Pt wire counter electrode, and an Ag/AgNO₃ reference electrode. The measurement was carried out under N₂ using *o*-dichlorobenzene (*o*-DCB) solution with 0.1 M tetrabutylammonium perchlorate (*n*-Bu₄N⁺ClO₄⁻) as a supporting electrolyte. The redox potentials were calibrated with ferrocene as an internal standard. The area of working electrode dipped into electrolyte solution is 1.0 cm × 1.5 cm.

The number of molecules adsorbed on a conducting surface can be estimated from CV by observing the dependency of the oxidative peak intensity on the scan rate as follows¹.

$$i_p = \frac{n^2 F^2}{4RTN_A} A \Gamma^* v \quad \square \square \quad \square \square \quad \square (1)$$

In the above equation, i_p (A) is the oxidative peak current, v ($V s^{-1}$) is the voltage scan rate, n is the number of electrons transferred, F ($96,485.33 C mol^{-1}$) is the Faraday constant, R ($8.3144 J K^{-1} mol^{-1}$) is the universal gas constant, T (K) is the temperature, N_A ($6.022 \times 10^{23} mol^{-1}$) is the Avogadro constant, A (cm^2) is the electrode surface area, and Γ^* ($molecules cm^{-2}$) is the surface density. The number of the adsorbed molecules per unit area can be determined experimentally by measuring the slope of i_p vs v .

4. Device fabrication

Materials

All materials were reagent grade and were used as received unless otherwise noted. Lead (II) iodide (PbI_2) and methylamine hydroiodide (MAI, $MA = CH_3NH_3$) were purchased from TCI. The syntheses of SAMs are described above. The ITO-coated glass ($2.5 \times 2.5 cm^2$, 0.7 mm, sheet resistance $\leq 10 \Omega/sq$) was Flat ITO purchased from GEOMATEC.

i-PSCs were prepared with the configuration ITO/SAM/perovskite/PCBM/ZnO/Ag. The HTL and perovskite layer were formed under dry atmospheric conditions, whereas the ETL layer was deposited under N_2 . HTLs were formed on ITO substrates by spin-coating SAMs in anhydrous ethanol (some concentrations described in main text) at 3000

rpm for 30 s, followed by heating on a hotplate at 100 °C for 10 min. $\text{Cs}_{0.05}(\text{FA}_{0.83}\text{MA}_{0.17})_{0.95}\text{Pb}(\text{I}_{0.83}\text{Br}_{0.17})_3$ perovskite layers were formed according to methods reported in the literature². For the perovskite precursor solution, FAI (0.9 M, Tokyo Chemical Industry), MABr (0.18 M, Tokyo Chemical Industry), PbI_2 (0.99 M, Tokyo Chemical Industry), and PbBr_2 (0.18 M, Tokyo Chemical Industry) were dissolved in a mixed solvent of anhydrous DMF (FUJIFILM Wako Chemicals) and anhydrous DMSO (FUJIFILM Wako Chemicals) (volume ratio of 4:1), and 4 vol% CsI (1.5 M, Tokyo Chemical Industry) in anhydrous DMSO was added. The perovskite precursor solution was spin-coated onto the ITO/SAM substrates through a two-step program of 1000 rpm for 10 s and 4000 rpm for 30 s. Anhydrous chlorobenzene (Sigma-Aldrich) was dropped onto the substrate 20 s before the end of spin coating to induce crystallization of the perovskite. The substrates were dried at 100 °C 60 min. To form the ETL, the substrates were transferred to a N_2 glovebox and [6,6]-Phenyl- C_{61} -butyric acid methyl ester (PCBM) (30 mg/mL, E102, Frontier Carbon) in anhydrous chlorobenzene was spin-coated at 4000 rpm for 30 s. ZnO (Sigma-Aldrich) in IPA (volume ratio of 1:1) was then spin-coated at 4000 rpm for 30 s. Finally, the Ag electrodes were formed via vapor deposition.

5. Solar cell performance measurements

Simulated AM 1.5 solar light was generated by a solar simulator (Bunkoukeiki, OTENTO-SUNV-SR with a 300 W Xe lamp and an AM 1.5 filter). $J-V$ curves were recorded using a direct-current voltage/current source meter (Keithley 2401). The incident light intensity was calibrated with a standard Si solar cell equipped with a KG-5 filter, which was fabricated by the Japan Quality Assurance Organization. The EQE spectra were acquired in ambient air at room temperature using an apparatus equipped with a Xe lamp and configured for acquiring action spectra (Bunkou Keiki HQE-25D).

6. Device stability test

A thermal stability test (65°C in ambient air, humidity was not controlled) was conducted in an environment testing tools apparatus manufactured by Asone (OF-300). After cooling to room temperature, the devices were measured quickly in the ambient air. All of the devices were encapsulated under N₂ and stored under dark conditions.

7. Characterization

UV–vis absorption spectra were acquired with a JASCO V-770 spectrophotometer with the samples in a quartz cuvette with a 10-mm path length. The concentration of each compound in DMF was 1×10^{-5} M. The redox potentials for the HTMs were obtained by DPV with an ALS 610B electrochemical analyzer using a three-electrode cell consisting of a glassy-carbon electrode, a Pt wire counter electrode, and a Ag/AgNO₃ reference electrode. The measurements were conducted using 0.1 M tetrabutylammonium perchlorate (TBAClO₄)–DMF sample solutions (1 mM). The potential was calibrated using the ferrocene/ferrocenium (Fc/Fc⁺) redox potential. Cross sections of solar cells were observed using a scanning electron microscope (Hitachi SU9000). Time-resolved PL was performed using a PL measurement system equipped with a time-correlated single-photon counting system (Fluorolog-QM, Horiba) at an excitation wavelength of 665 nm.

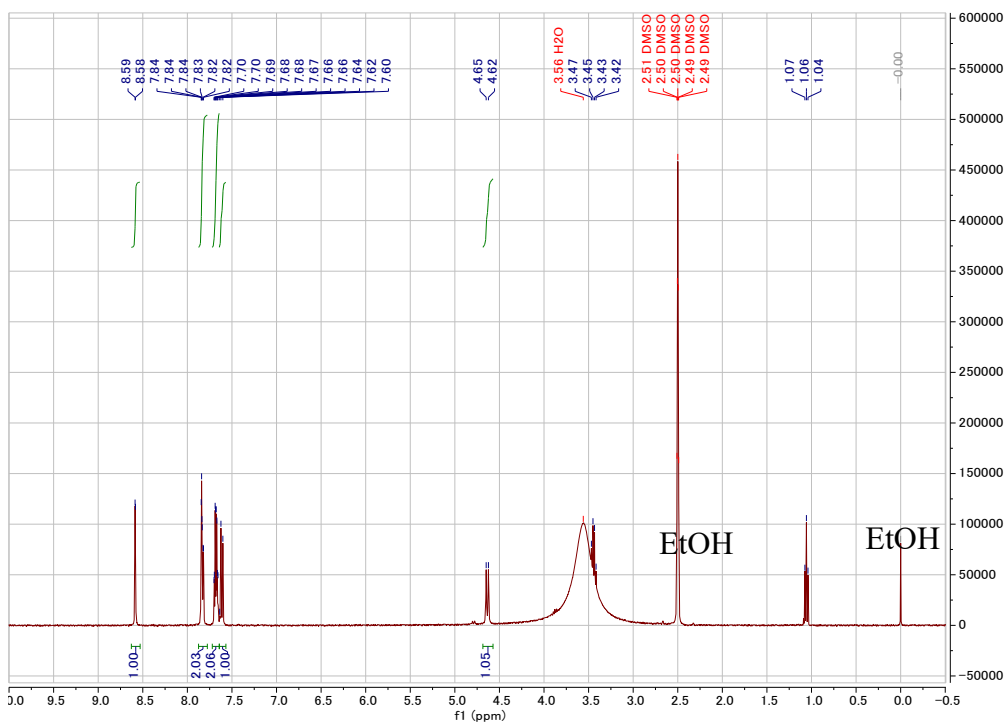


Fig. S1 ^1H NMR spectrum of T-PACz in $\text{DMSO-}d_6$.

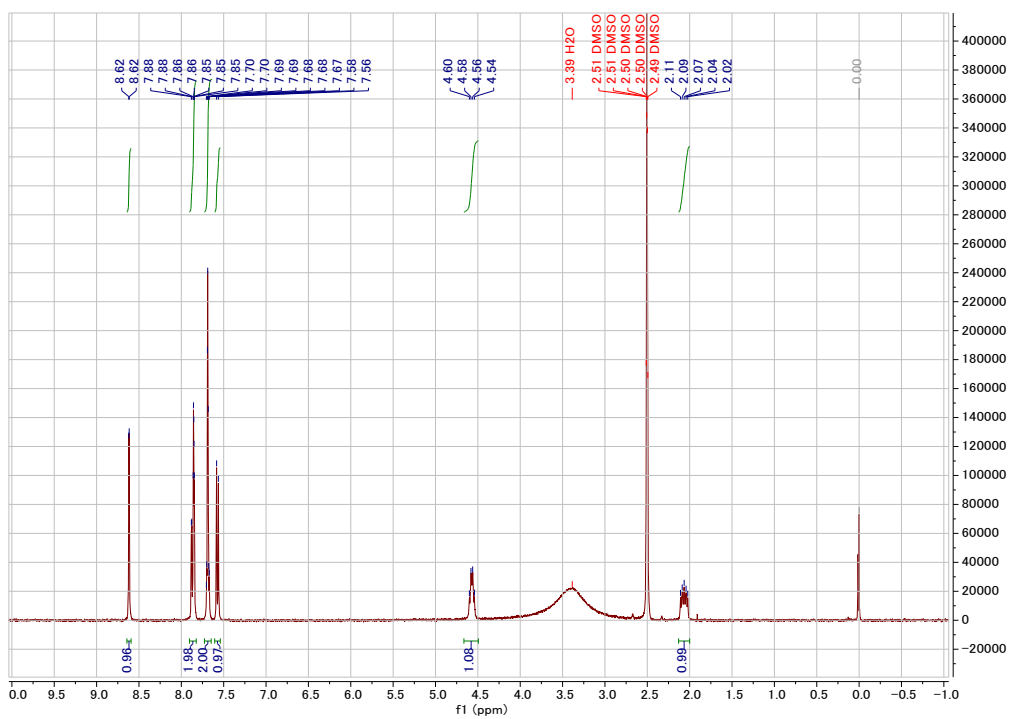


Fig. S2 ^1H NMR spectrum of T-2PACz in $\text{DMSO-}d_6$.



Fig. S3 ¹H NMR spectrum of T-3PACz in DMSO-*d*₆.

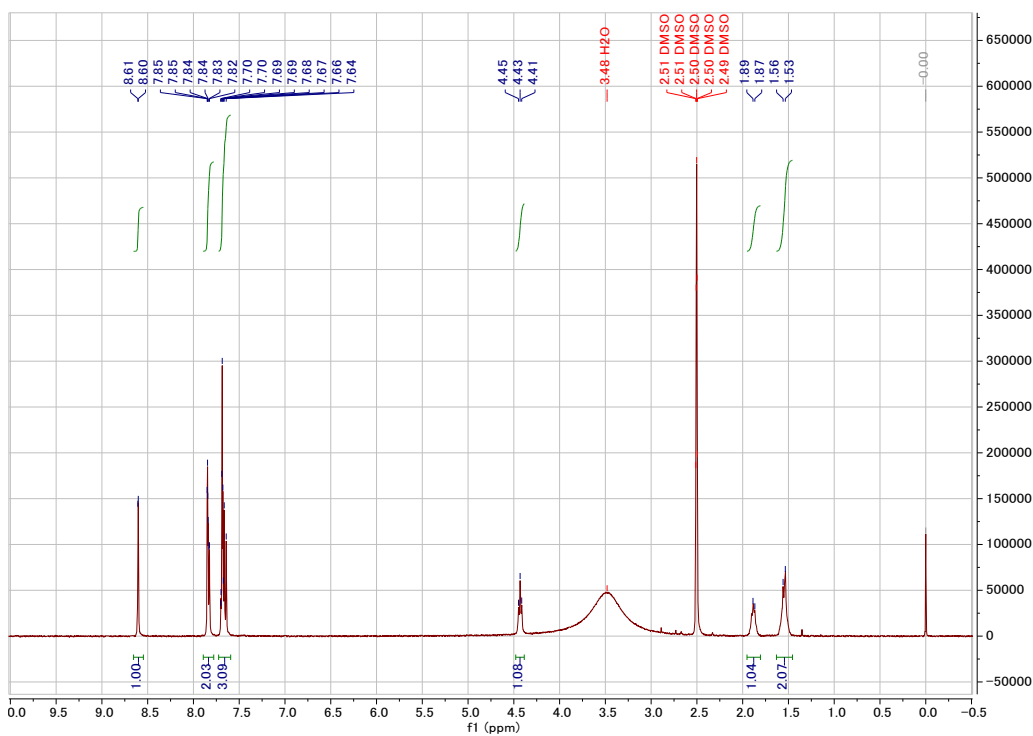


Fig. S4 ¹H NMR spectrum of T-4PACz in DMSO-*d*₆.

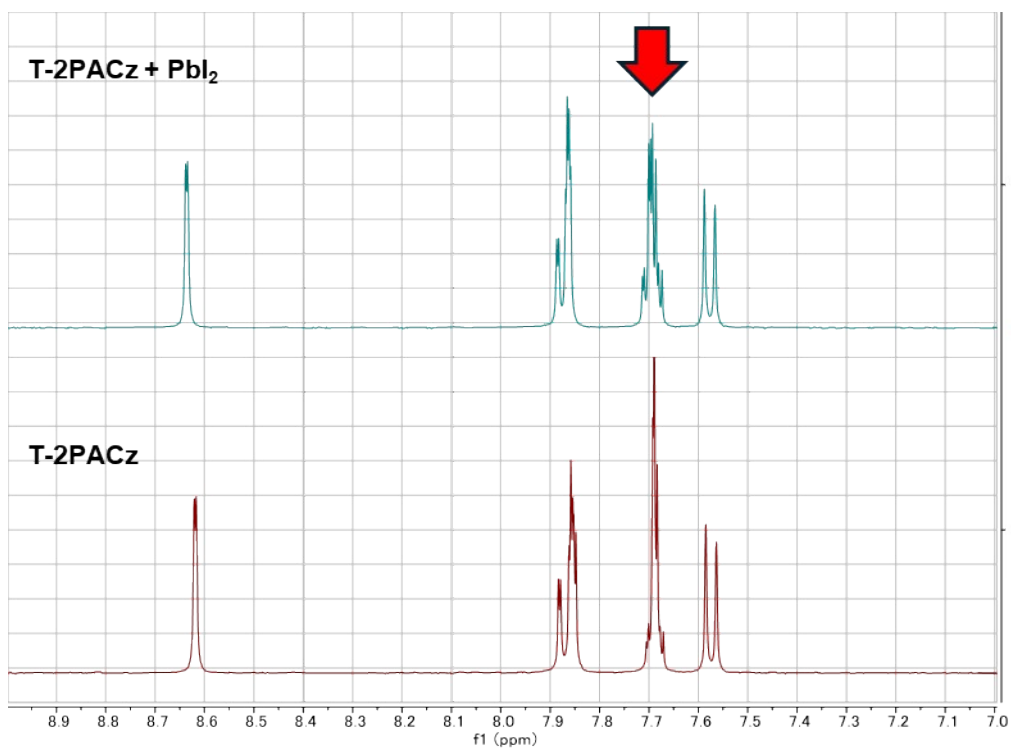


Fig. S5 Comparison of ¹H NMR spectrum of T-2PACz and T-2PACz treated with PbI₂ in DMSO-*d*₆.

Table S1. Optical and electrochemical properties of HTMs.

SAM	λ_{\max} (nm) ^a	λ_{onset} (nm)	$E_{\text{g}}^{\text{opt}}$ (eV) ^b	E_{HOMO} (eV) ^c	E_{LUMO} (eV) ^d
2PACz	332, 346	354	3.50	-5.60	-2.10
T-PACz	354, 370-375sh	388	3.20	-5.36	-2.16
T-2PACz	354, 370-375sh	384	3.23	-5.37	-2.14
T-3PACz	354, 370-375sh	384	3.23	-5.35	-2.12
T-4PACz	354, 370-375sh	384	3.23	-5.34	-2.11

^aMeasured in DMF solution with a concentration of 10^{-5} M.

^bEstimated from the absorption edge in solution using the equation $E_{\text{g}}^{\text{opt}} = 1240/\lambda_{\text{onset}}$ (eV).

^c E_{HOMO} was estimated by DPV method in DMF.

^d E_{LUMO} was estimated by the equation $E_{\text{LUMO}} = E_{\text{HOMO}} + E_{\text{g}}^{\text{opt}}$.

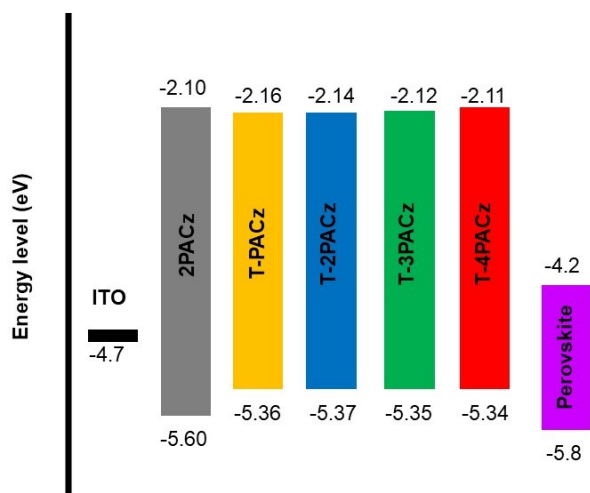


Fig. S6 Energy diagram for SAMs. The value for perovskite was obtained from PYS and UV spectra.

Table S2. Photovoltaic Parameters of i-PSCs based on SAMs

(a) Forward Scan

SAM ^a	J_{sc} (mA cm ⁻²)	V_{oc} (V)	FF	PCE (%)
2PACz	20.2 ± 0.4^b	1.09 ± 0.01	0.63 ± 0.03	14.0 ± 0.8
	(20.9) ^c	(1.10)	(0.70)	(16.0)
T-PACz	20.1 ± 0.5^b	1.07 ± 0.03	0.67 ± 0.04	14.5 ± 1.3
	(20.3) ^c	(1.08)	(0.73)	(15.8)
T-2PACz	19.9 ± 0.8^b	1.06 ± 0.01	0.68 ± 0.04	14.3 ± 1.2
	(21.1) ^c	(1.05)	(0.72)	(15.9)
T-3PACz	20.2 ± 0.5^b	1.07 ± 0.01	0.68 ± 0.05	14.8 ± 1.1
	(20.6) ^c	(1.08)	(0.73)	(16.2)
T-4PACz	20.2 ± 0.4^b	1.08 ± 0.01	0.71 ± 0.03	15.4 ± 0.9
	(20.9) ^c	(1.09)	(0.74)	(16.9)

(b) Backward Scan

SAM ^a	J_{sc} (mA cm ⁻²)	V_{oc} (V)	FF	PCE (%)
2PACz	20.4 ± 0.4 ^b	1.09 ± 0.01	0.65 ± 0.03	14.4 ± 1.0
	(21.3) ^c	(1.10)	(0.71)	(16.6)
T-PACz	20.2 ± 0.4 ^b	1.07 ± 0.03	0.66 ± 0.05	14.1 ± 1.4
	(20.8) ^c	(1.06)	(0.74)	(16.3)
T-2PACz	19.9 ± 0.7 ^b	1.06 ± 0.02	0.66 ± 0.04	13.9 ± 1.3
	(20.9) ^c	(1.07)	(0.73)	(16.4)
T-3PACz	20.2 ± 0.5 ^b	1.07 ± 0.02	0.66 ± 0.05	14.3 ± 1.3
	(21.2) ^c	(1.06)	(0.73)	(16.5)
T-4PACz	20.3 ± 0.4 ^b	1.07 ± 0.02	0.68 ± 0.03	14.7 ± 0.9
	(20.5) ^c	(1.09)	(0.72)	(16.0)

^a SAM concentration was 2 mM in EtOH. ^b These values were obtained from 24-31 solar cells and are reported as the average ± standard deviation. ^c Values obtained from the best-performing solar cell.

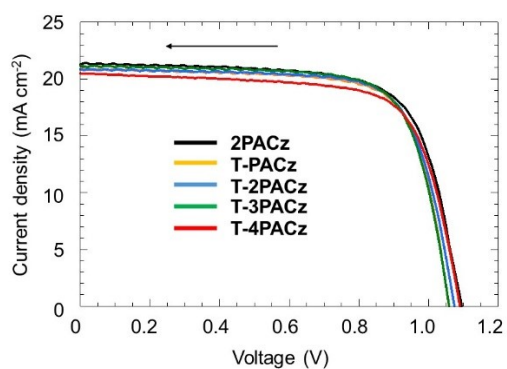


Fig. S7 J - V curves for the PSCs based on SAMs, as measured by backward scans. □

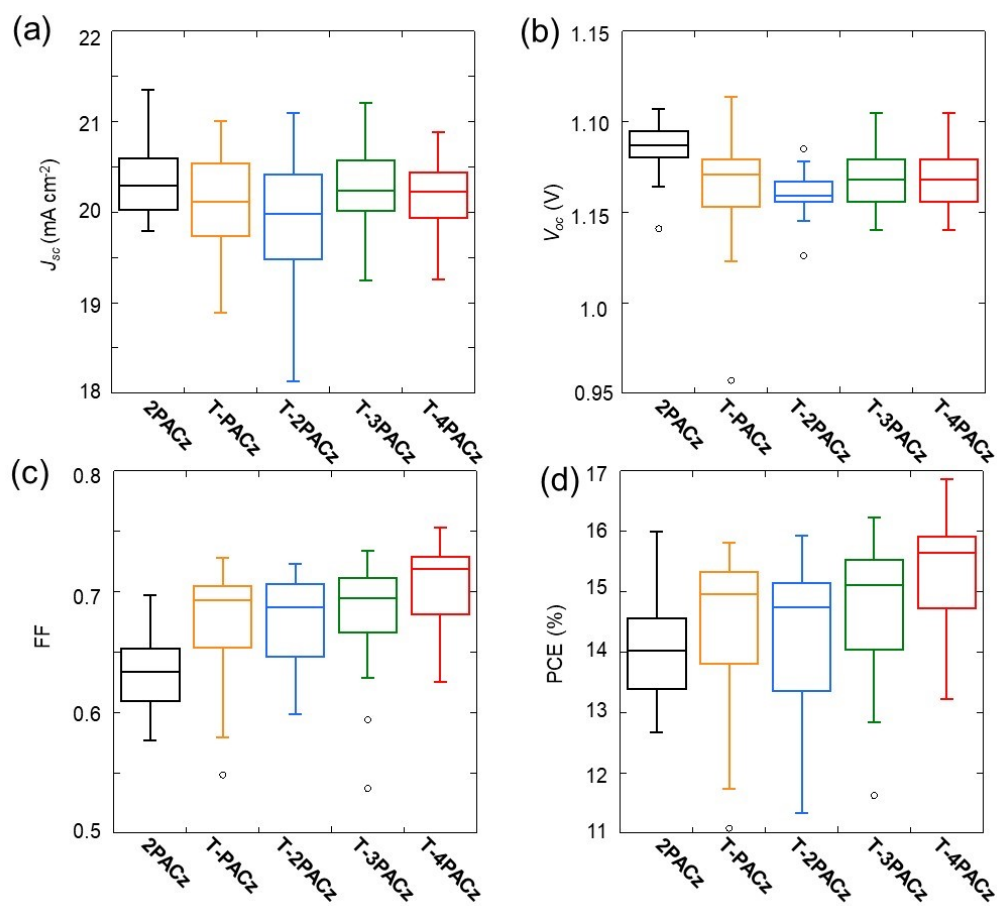


Fig. S8 Box plots of (a) J_{sc} , (b) V_{oc} , (c) FF, and (d) PCE of the PSCs based on SAMs with 2 mM precursor in EtOH solutions obtained in the forward scan.

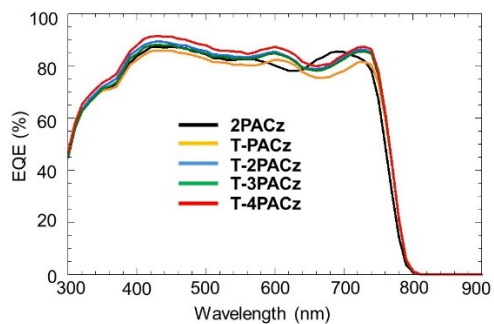


Fig. S9 EQE spectra for the PSCs based on SAMs. □

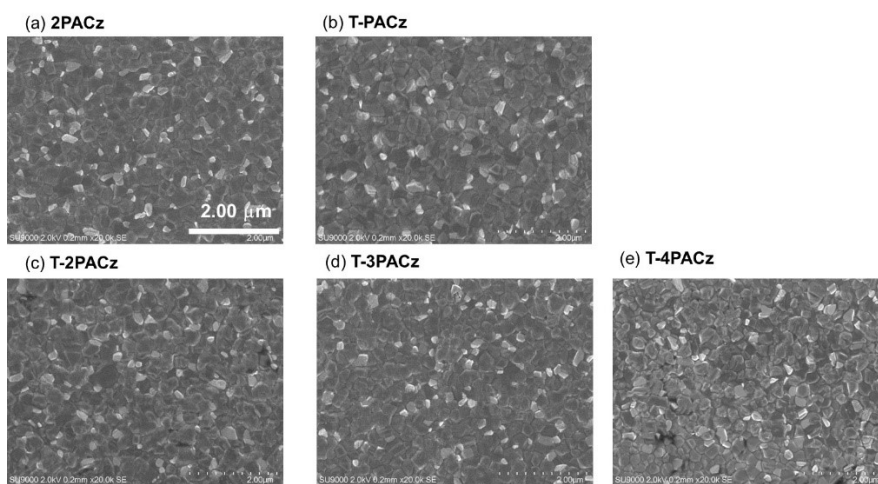


Fig. S10 Top view of perovskite based on SAMs. □

Table S3. Time-Resolved PL Measurements.

Sample	τ_1 (ns)	Intensity	τ_2 (ns)	Intensity	Average (ns)
ITO/Perovskite	2.4	<0.01	52.0	1	52.0
ITO/2PACz	4.7	0.01	32.8	0.99	32.6
ITO/T-PACz	2.5	0.01	21.7	0.99	21.5
ITO/T-2PACz	1.6	0.38	12.7	0.62	8.5
ITO/T-3PACz	1.9	0.39	16.8	0.61	9.8
ITO/T-4PACz	1.5	0.41	15.8	0.59	9.9

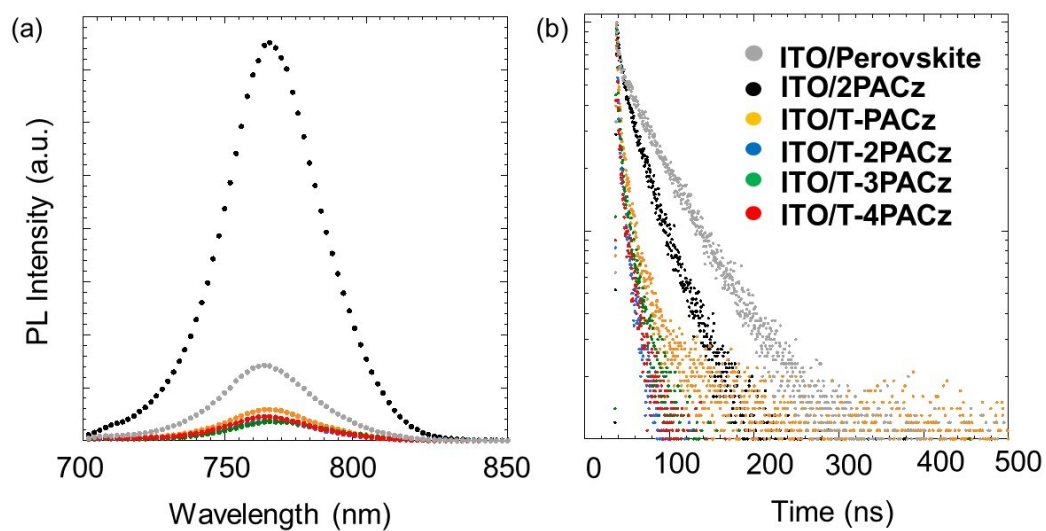
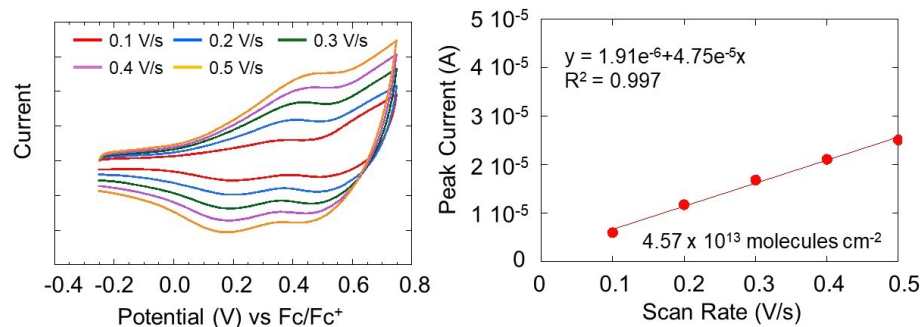
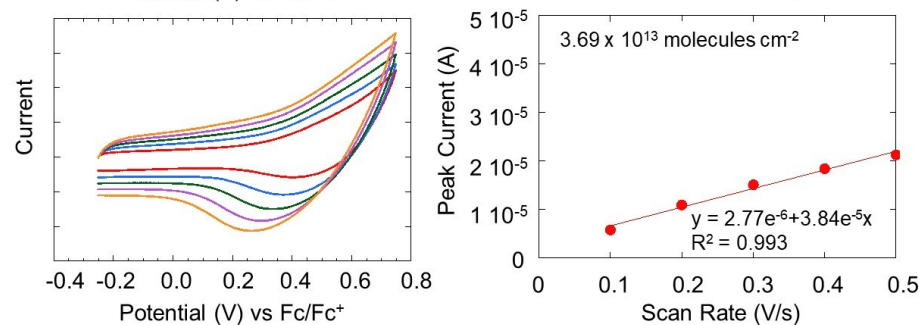
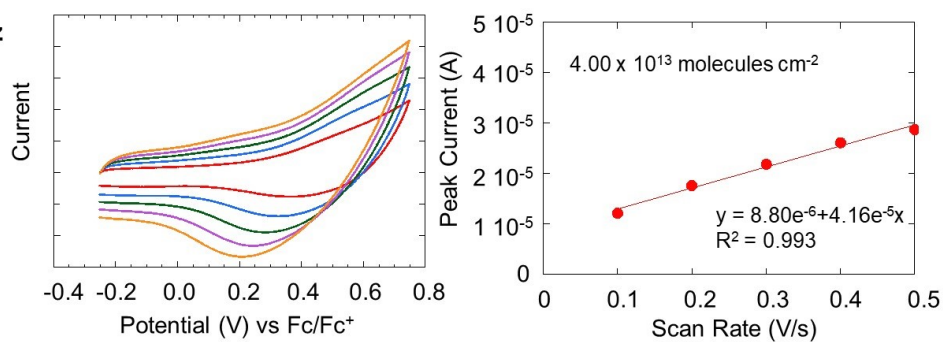
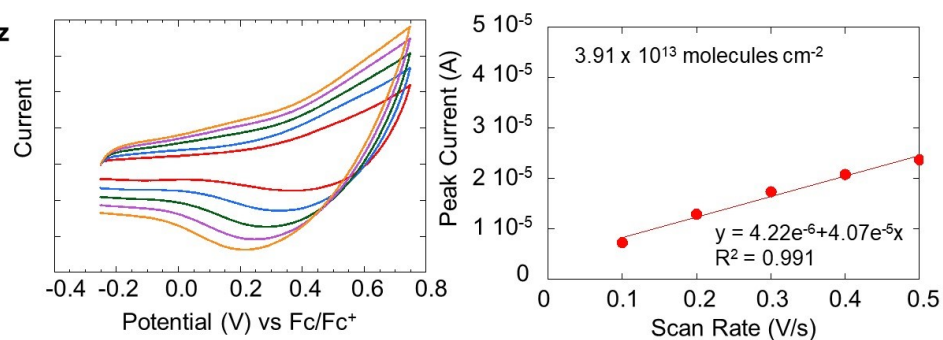


Fig. S11 (a) Steady-state PL intensity and (b) TRPL decay curves for ITO/SAM/perovskite structures.

2PACz**T-PACz****T-2PACz****T-3PACz**

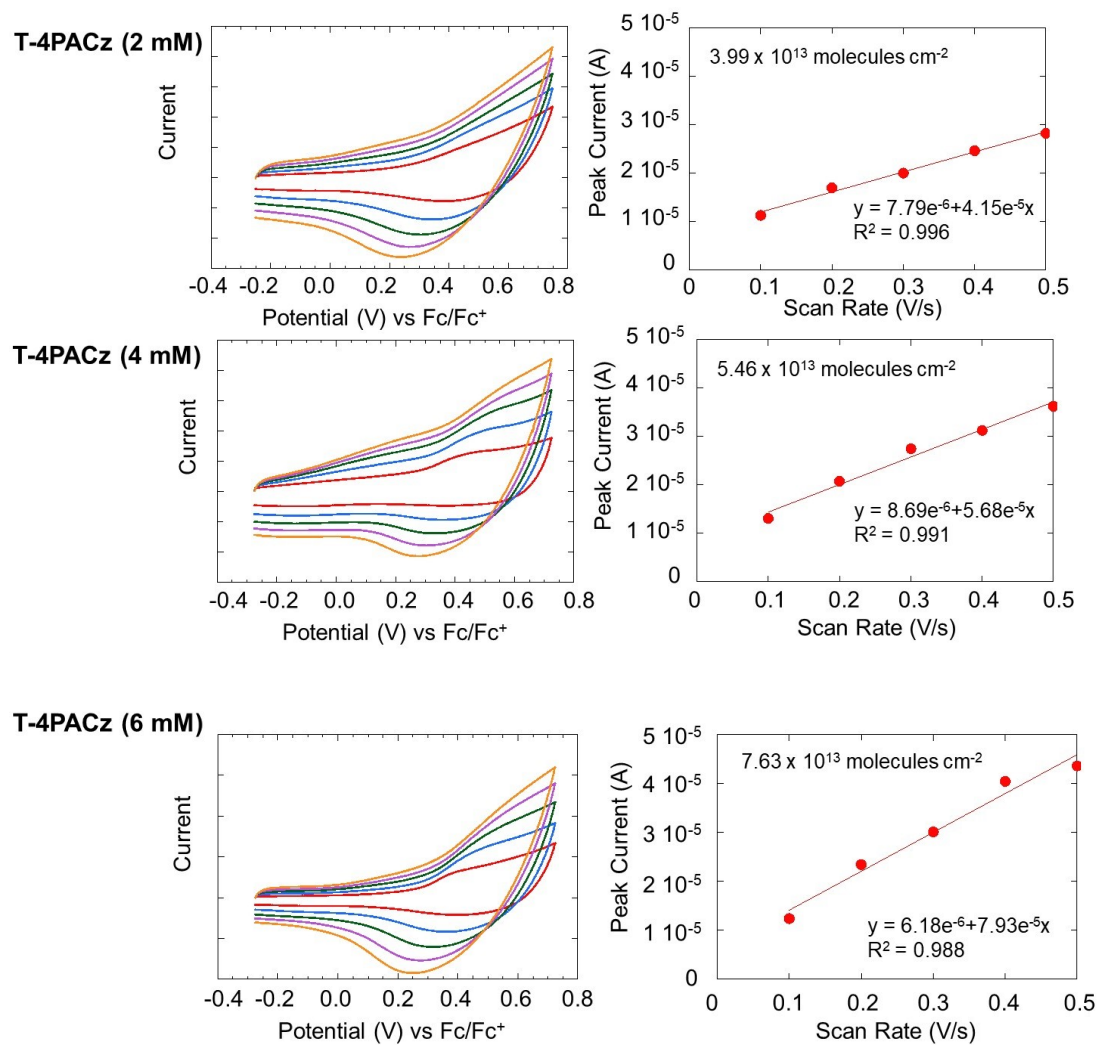


Fig. S12 CVs of the SAMs adsorbed on ITO substrates measured in *o*-DCB solution under different scan rates and their corresponding peak current vs scan rate chart.

Table S4. Adsorbed molecules on ITO

SAM	Concentration (mM)	Molecules (cm ⁻²)
2PACz	2	4.57 x 10 ¹³
T-PACz	<2	3.69 x 10 ¹³
T-2PACz	2	4.00 x 10 ¹³
T-3PACz	<2	3.91 x 10 ¹³
T-4PACz	2	3.99 x 10 ¹³
T-4PACz	4	5.46 x 10 ¹³
T-4PACz	6	7.63 x 10 ¹³

Table S5 Photovoltaic Parameters of PSCs based on **T-4PACz**.^a

(a) Forward scan

Concentration of T-4PACz (in EtOH)	J_{sc} (mA cm ⁻²)	V_{oc} (V)	FF	PCE (%)
1 mM	19.8 ± 0.5 ^b (20.6) ^c	1.06 ± 0.01 (1.09)	0.65 ± 0.05 (0.75)	13.7 ± 1.5 (16.7)
2 mM	20.2 ± 0.4 (20.9)	1.08 ± 0.01 (1.09)	0.71 ± 0.03 (0.74)	15.4 ± 0.9 (16.9)
4 mM	20.7 ± 0.3 (20.8)	1.07 ± 0.01 (1.09)	0.72 ± 0.02 (0.76)	16.0 ± 0.7 (17.3)
6 mM	20.5 ± 0.5 (21.0)	1.07 ± 0.01 (1.09)	0.70 ± 0.03 (0.75)	15.4 ± 0.9 (17.1)

(b) Backward scan

Concentration of T-4PACz (in EtOH)	J_{sc} (mA cm ⁻²)	V_{oc} (V)	FF	PCE (%)
1 mM	19.9 ± 0.5 ^b (20.8) ^c	1.06 ± 0.01 (1.09)	0.63 ± 0.05 (0.74)	13.4 ± 1.3 (16.7)
2 mM	20.3 ± 0.4	1.07 ± 0.02	0.68 ± 0.03	14.7 ± 0.9

	(20.5) ^c	(1.09)	(0.72)	(16.0)
4 mM	20.7 ± 0.3 ^b	1.07 ± 0.01	0.72 ± 0.03	16.1 ± 0.8
	(20.9) ^c	(1.09)	(0.77)	(17.4)
6 mM	20.6 ± 0.4	1.07 ± 0.01	0.68 ± 0.03	15.1 ± 0.9
	(20.9) ^c	(1.08)	(0.75)	(16.9)

^a These values were obtained from 20–23 solar cells by forward scan. ^b These values are reported as the average ± standard deviation. ^c Values obtained for the best-performing solar cell.

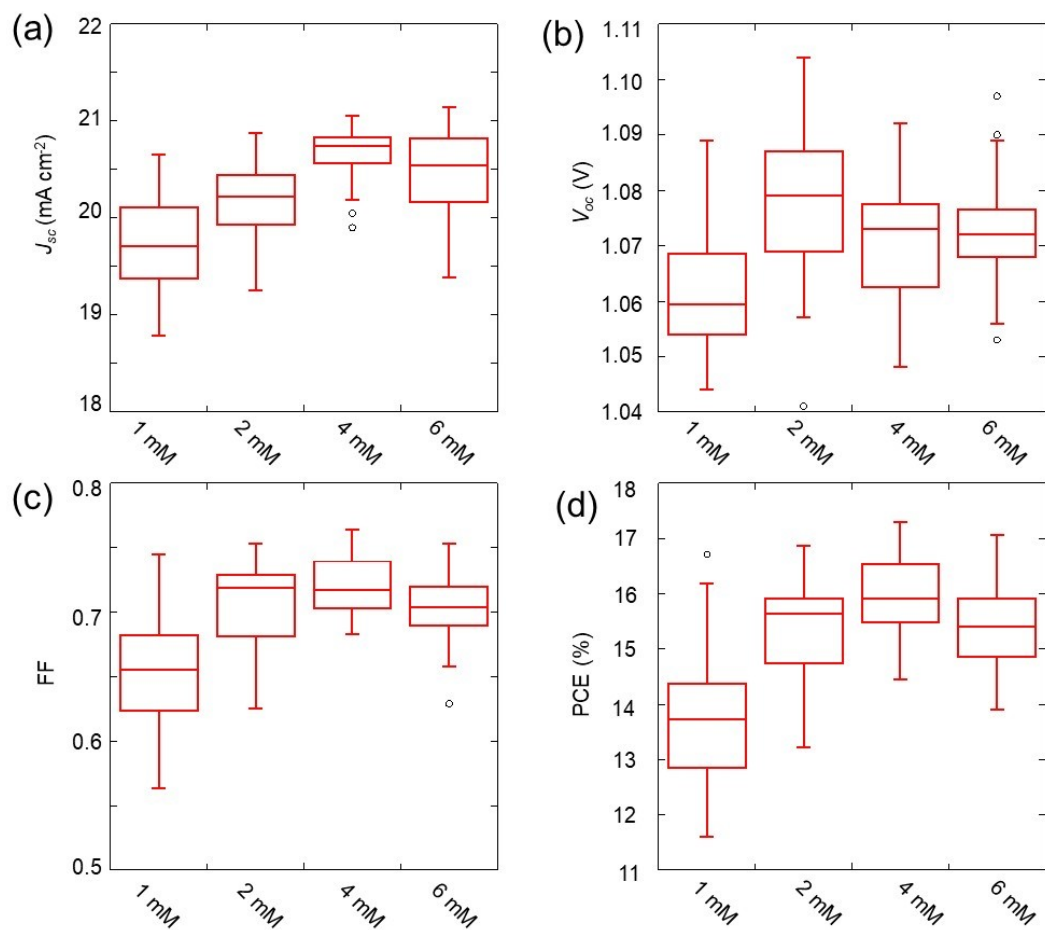


Fig. S13 Box plots of (a) J_{sc} , (b) V_{oc} , (c) FF and (d) PCE of the PSCs based on T-4PACz with various concentration precursors in EtOH solutions obtained in the forward scan.

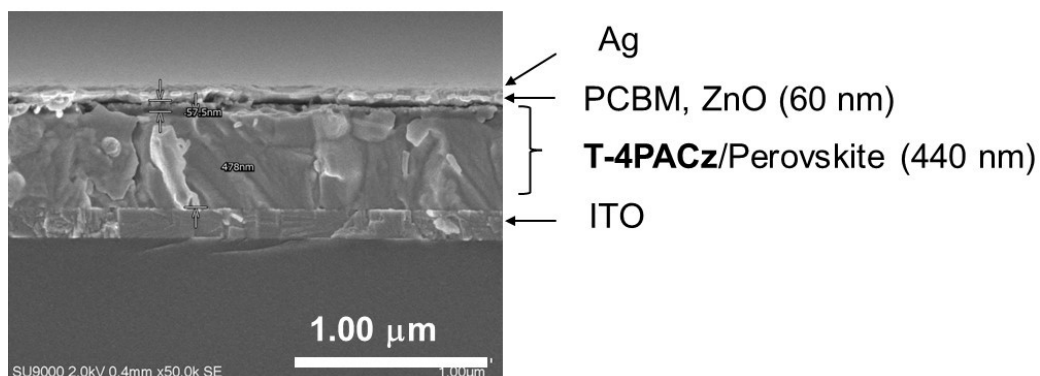


Fig. S14 Cross-sectional SEM image based on T-4PACz (4 mM in EtOH).

Reference

1. M. A. Truong, T. Funasaki, L. Ueberricke, W. Nojo, R. Murdey, T. Yamada, S. Hu, A. Akatsuka, N. Sekiguchi, S. Hira, L. Xie, T. Nakamura, N. Shioya, D. Kan, Y. Tsuji, S. Iikubo, H. Yoshida, Y. Shimakawa, T. Hasegawa, Y. Kanemitsu, T. Suzuki and A. Wakamiya, *J Am Chem Soc*, 2023, 145, 7528-7539.
2. A. Kogo, R. Ishikawa and T. N. Murakami, *ACS Applied Energy Materials*, 2024, 7, 7769-7774.